Review

# Recent insights into eukaryotic double-strand DNA break repair unveiled by single-molecule methods

Sara De Bragança,[1] Mark S. Dillingham,[2] and Fernando Moreno-Herrero [ID] [1,*]

Genome integrity and maintenance are essential for the viability of all organisms. A wide variety of DNA damage types have been described, but double-strand breaks (DSBs) stand out as one of the most toxic DNA lesions. Two major pathways account for the repair of DSBs: homologous recombination (HR) and non-homologous end joining (NHEJ). Both pathways involve complex DNA transactions catalyzed by proteins that sequentially or cooperatively work to repair the damage. Single-molecule methods allow visualization of these complex transactions and characterization of the protein:DNA intermediates of DNA repair, ultimately allowing a comprehensive breakdown of the mechanisms underlying each pathway. We review current understanding of the HR and NHEJ responses to DSBs in eukaryotic cells, with a particular emphasis on recent advances through the use of single-molecule techniques.

## DNA double-strand break repair

DSBs not only arise spontaneously due to replicative stress in all dividing cells but can also be induced by exposure to ionizing radiation or chemotherapeutic agents. Timely and faithful repair of DSBs is imperative for the maintenance of genome integrity as failure to do so leads to mutagenesis or loss of genetic information [1,2]. The DNA damage response (DDR) is composed of several repair pathways that together ensure high-fidelity repair of DSBs. Mutations in DDR effectors are implicated in human genetic disease and cancer [3]. There are two major pathways for DNA repair which differ in their requirement for a homologous template DNA to direct repair: NHEJ and HR. The NHEJ pathway is fast, and is completed in ~30 min [4], but is also potentially mutagenic owing to the low-fidelity end processing that may be required to make ends compatible for repair, leading to undesired localized insertions or deletions [2,5]. The HR pathway is slower, taking 7 h or longer to complete [4], but potentially repairs DNA with high fidelity. This reflects the use of a homologous DNA molecule (typically the sister chromatid) as the template for repair, and also restricts this process to the S and G2 phases of the cell cycle. It is now also appreciated that NHEJ and HR are not mutually exclusive and that repair may in some cases be directed by hybrid pathways, a situation that may be especially significant when some repair factors are dysfunctional in disease states [6]. The main protein components acting in the repair pathways have already been identified and to some extent characterized [1,2,7–15]. However, many questions remain concerning how the activities of these proteins are regulated and coordinated in space and time to ensure that DSBs are efficiently repaired by the optimum available pathway.

In the past few years single-molecule techniques have made an increasingly important contribution to our mechanistic understanding of the DDR because of their ability to directly visualize the dynamic interactions between damaged DNA and the protein complexes that direct their repair [5,16–18]. These methods bypass many complexities of bulk analyses by allowing the study of

## Highlights

Single-molecule methods allow real-time visualization of protein:DNA interactions, enabling detailed investigation of DNA damage repair.

Intermediate repair stages are revealed from unsynchronized populations using single-molecule methods, thus elucidating the dynamics and mechanisms of DNA repair.

Single-molecule methods have provided novel mechanistic insights into the molecular motors and protein machines involved in eukaryotic double-strand DNA break repair.

[1]Department of Macromolecular Structures, Centro Nacional de Biotecnología (CNB), CSIC, Madrid, Spain
[2]DNA:Protein Interactions Unit, School of Biochemistry, University of Bristol, Bristol BS8 1TD, UK

*Correspondence:
fernando.moreno@cnb.csic.es
(F. Moreno-Herrero).

individual enzymatic reactions in unsynchronized populations. In combination with biochemical reconstitution of the DNA repair process using purified components, these approaches allow researchers to better define the protein:DNA intermediates of DNA repair and the kinetics of the transitions between them, ultimately allowing complete mechanistic dissection of each pathway.

In this review we discuss current understanding of the HR (up to the strand-invasion step) and NHEJ responses to DSBs in eukaryotic cells, focusing on recent progress using single-molecule techniques including optical tweezers, magnetic tweezers, single-molecule fluorescence resonance energy transfer (smFRET), DNA curtains, and atomic force microscopy (AFM). We have also included recent insights from cryogenic electron microscopy (cryo-EM; a powerful complementary approach to single-molecule methods) which has illuminated important structural aspects of DNA repair (Box 1). An exhaustive review of DNA repair pathways is beyond the scope of this work, and we recommend other recent publications [1–3,8,19,20].

## Homologous recombination
### DSB detection and initiation of the HR pathway
The HR pathway is intrinsically complex and involves a multitude of proteins and several perfectly synchronized stages (Figure 1 and Table 1). It is restricted to the S and G2 phases of the cell

---

**Box 1. Single-molecule methods to study DNA double-strand break repair**

In a typical atomic force microscopy (AFM) setup (Figure IA), the molecules of interest are adsorbed onto a flat surface and an oscillating cantilever with a nanometer-sized tip scans over the surface. The movement of the oscillating tip is measured using a laser beam that is reflected at the back of the cantilever and directed to a photodiode. The interaction of the tip with the sample affects the amplitude of the oscillation, and by keeping this amplitude constant along the scan a 3D image can be reconstructed. AFM instruments can be operated in a liquid environment with sufficient resolution to visualize individual proteins and nucleic acids at sub-second imaging rates.

In a DNA curtains setup (Figure IB), many DNA molecules are immobilized at one or both ends on the lower surface of a microfluidic chamber. In the case of single-tethered DNAs, application of a flow parallel to the surface extends the molecules. Depending on the biological system under study, either the DNA molecules or the proteins of interest, or both, are labeled with DNA intercalants or fluorophores. The visualization of the labeled molecules is based on total internal reflection fluorescence (TIRF) microscopy where only the emission from the particles near the surface is detected. This method is useful to visualize DNA:protein binding events and protein movement on DNA with a resolution limited by diffraction, ~200–300 nm.

In a combined optical tweezers and confocal fluorescence microscopy setup (Figure IC), a DNA molecule is immobilized in solution between two optically trapped beads. The molecule can be stretched or relaxed depending on the distance between traps, and the force applied to the molecule can be calculated from the displacements of the optically trapped beads with respect to the center of the trap. Depending on the experiment, DNA or proteins, or both, can be fluorescently labeled. The visualization of the labeled molecules is based on confocal microscopy in which an excitation laser is scanned along the experimental area while the emitted photons are collected. This setup facilitates the visualization of a wide variety of DNA–protein interactions and can correlate protein binding and movement on DNA with transitions in DNA structure such as duplex unwinding (Figure IC). Typical forces in these experiments range from ~1 to 100 pN, and proteins can be localized with a resolution limited by diffraction, ~200–300 nm.

Single-molecule fluorescence resonance energy transfer (smFRET) assays (Figure ID) employ a pair of fluorophores with overlapping emission and excitation spectra, from donor and acceptor, respectively (e.g., Cy3 and Cy5). Excitation of the donor fluorophore results in the nonradiative transfer of energy to the acceptor fluorophore which can be detected as an increase in acceptor emission. Because the efficiency of energy transfer between fluorophores is distance-dependent within a 1–10 nm range, this technique has proved to be useful for studying DNA:protein binding and associated conformational changes, as well as protein-mediated DNA bridging (Figure ID).

In a magnetic tweezers setup (Figure IE), a microfluidic chamber is placed above an inverted microscope and below a pair of magnets and a source of light. In the microfluidic chamber, multiple DNA molecules are tethered between the lower surface and a superparamagnetic bead which is attracted towards the magnetic field produced by a pair of permanent magnets. In this manner, the DNA molecules can not only be stretched or relaxed depending on the force applied but can also be supercoiled or unwound by applying positive or negative rotations. This technique is useful for studying protein-mediated changes in DNA structure that affect its extension, including dsDNA unwinding, rewinding, supercoiling, or condensation, as well as protein-mediated DNA bridging or looping (Figure IE). Typical forces in these experiments range from ~0.1 to 30 pN. Changes in the extension of the DNA tether can be determined within a few to tens of nanometers depending on the stretching force.

In cryo-electron microscopy (cryo-EM; Figure IF), the sample of interest is deposited onto a mesh and vitrified by rapid cooling. The non-crystalline frozen sample is then bombarded with electrons and those that go through the sample are collected onto an electron detector. The resulting images show randomly oriented 2D projections of the particles within the frozen sample. Computational processing transforms these projections into density maps that reveal the 3D structures of protein/complexes and the intra/inter-molecule interactions. Cryo-EM can resolve the atomic structure of proteins and nucleic acids, and is a powerful complementary technique to single-molecule methods because it provides mechanistic insights into the function of proteins. Additional details on the single-molecule methodologies described here can be found in [102–107].
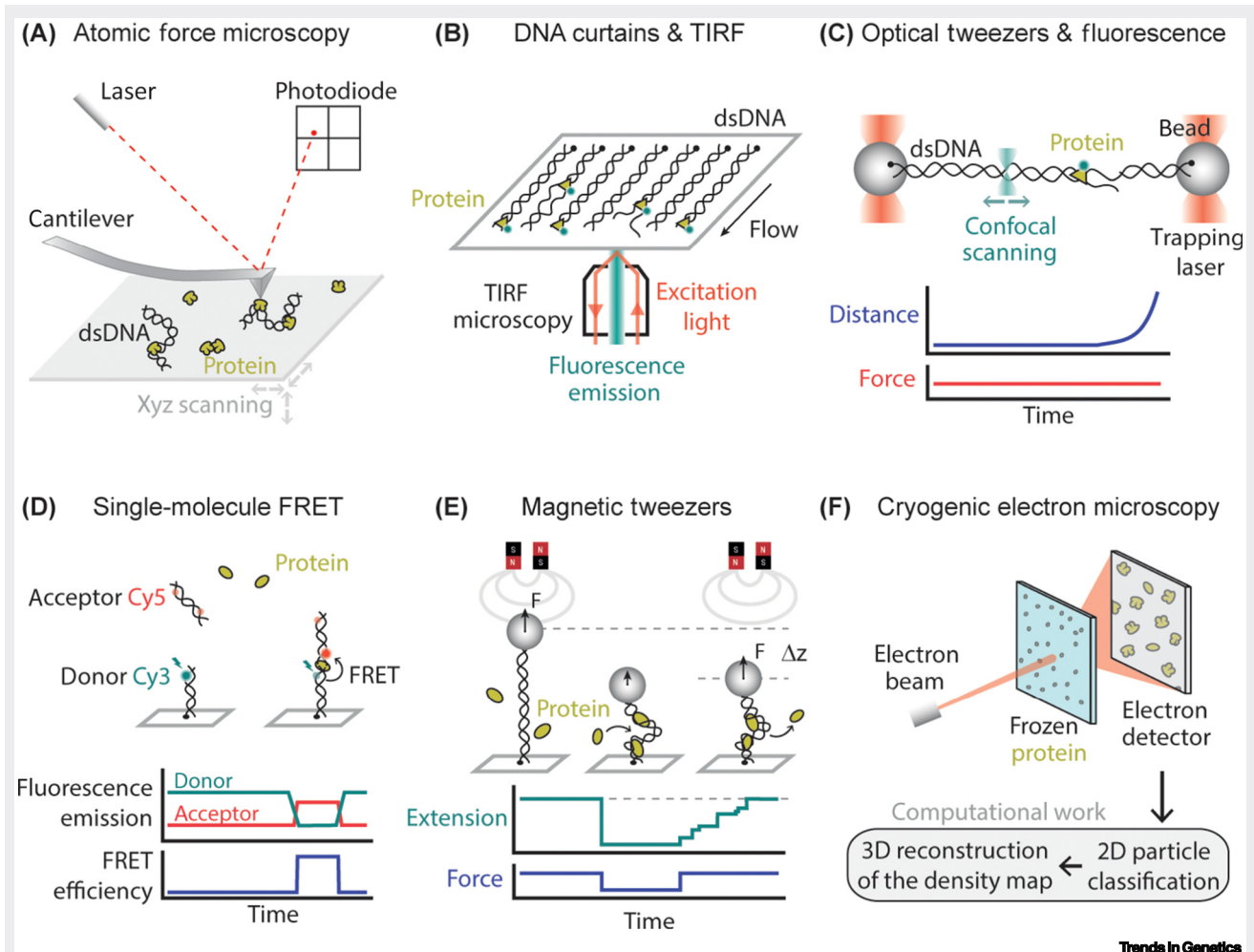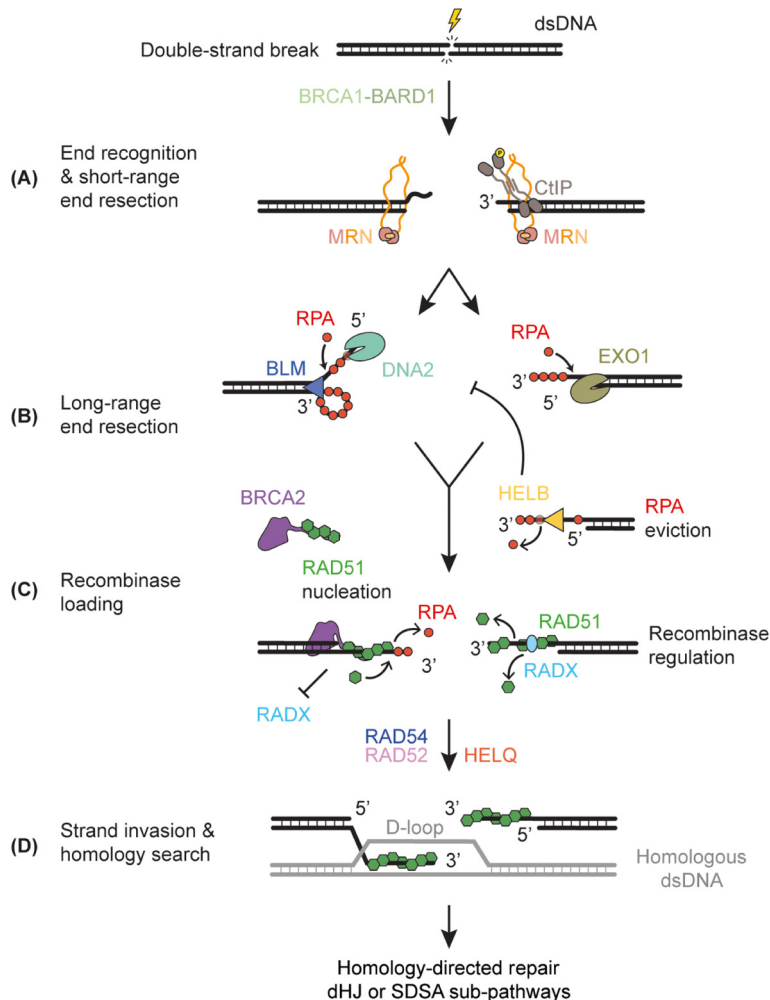
Figure I. Illustration of single-molecule methods and cryo-EM. Abbreviations: ds, double strand; FRET, fluorescence resonance energy transfer; TIRF, total internal reflection fluorescence.

cycle, and is predominant only during S phase [21]. Upon formation of a DSB, the MRE11-RAD50-NBS1 complex (MRN) localizes at the break site and activates ATM (Tel1 in yeast) that orchestrates a signaling cascade [14,22]. This response promotes the accumulation of the NHEJ positive regulator 53BP1 at the damaged chromatin. Among other functions, 53BP1 protects the break site against resection [14,23,24]. A positive feedback loop caused by the accumulation of 53BP1 and cofactors amplifies ATM activity [14]. During the S and G2 phases, the BRCA1-BARD1 complex antagonizes 53BP1, inhibiting NHEJ and enabling end resection, thereby initiating the HR pathway [23,25]. This effect of BRCA1-BARD1 in promoting HR is amplified by the activation of its interaction partner CtIP by cyclin-dependent kinases (CDKs), which in turn triggers MRN cleavage events that initiate resection (discussed later) [26].

### End recognition and short-range end resection
MRN and CtIP (Sae2 in yeast) cooperate to perform short-range resection of the DNA ends and remove secondary DNA structures and DNA-bound protein blocks [10,27] (Figure 1A). It was

**Figure 1. Cartoon showing early steps of the homologous recombination (HR) pathway.** (A) End recognition and short-range end resection. The HR repair pathway initiates when BRCA1-BARD1 and MRN localize at the site of the double-strand break (DSB) and recruit the cofactor CtIP. MRN and CtIP then perform short-range resection that removes complex secondary structures and/or protein blocks from the DNA ends. (B) Long-range resection. This stage is performed by the nucleases EXO1 or nuclease/helicase DNA2 with assistance from the helicases BLM or WRN. This prepares the DNA ends for the downstream homology search and results in long 3′ ssDNA overhangs. As soon as the ssDNA tracks are exposed, RPA recognizes and binds, efficiently covering the entire ssDNA overhang. (C) Recombinase loading. This stage results in the replacement of RPA by the recombinase RAD51. RAD51 forms a nucleoprotein filament around the ssDNA tail and, although it can evict RPA from the ssDNA overhangs, this exchange is only efficient in the presence of positive mediators such as BRCA2. In turn, negative mediators such as RADX regulate filament formation. HELB efficiently evicts RPA from ssDNA and inhibits long-range resection. (D) Strand invasion and homology search. The recombinase RAD51 is responsible for this stage, which is mediated by several factors, such as RAD54, RAD52, and HELQ. Finally, HR polymerases drive template-based synthesis of the 3′ end. The repair pathway continues by either (i) the double Holliday junction sub-pathway (dHJ) in which the second end is captured and a double Holliday junction is formed and resolved, or by (ii) the synthesis-dependent single-strand annealing sub-pathway (SDSA), in which the invading strand unbinds from the donor through branch migration, and this newly extended 3′ strand anneals with the second end through complementary base pairing. Abbreviations: dsDNA, double-stranded DNA; MRN, MRE11-RAD50-NBS1 complex; RPA, replication protein A; ssDNA, single-stranded DNA.

Table 1. HR factors addressed in this review

| Eukaryotic[a] | Function | Refs |
|---|---|---|
| BRCA1-BARD1 | HR promoter | [23,25,26,28] |
| MRE11-RAD50-NBS1 (MRN) | Nuclease<br>Structural role<br>DSB sensor | [7,10,14,22,26–30,36–38,40–43] |
| CtIP | MRN activation<br>DNA bridging<br>Regulation | [7,10,26–28,31–34,36–39,44,45] |
| EXO1 | Exonuclease | [28,37,40–43,46,59] |
| DNA2 | Helicase,<br>Nuclease | [28,40–42,44–46,59] |
| BLM | Helicase | [28,40–43,45–48,59] |
| WRN | Helicase | [40,41] |
| RPA | ssDNA-binding protein<br>ssDNA protection | [9,11,40,41,44,46–48,52,54–56,58,60–63,71] |
| RAD51 | Recombinase | [9,11,13,51–57,60–63,71,92] |
| RAD52 | Positive recombinase mediator | [9,11,13,53,63,65] |
| BRCA2 | Positive recombinase mediator | [9,11,54–56] |
| Rad55-Rad57 (yeast) | Rad51 paralogs | [57] |
| HELB | Translocase<br>Strand-exchange promoter<br>Resection inhibitor | [58,59] |
| RADX | Negative recombinase mediator | [60,61] |
| RAD54 | Chromatin remodeler<br>Stimulates D-loop formation | [13,66,67] |
| Srs2 (yeast) | Negative recombinase mediator | [62,63] |

[a]All the proteins listed are human except those indicated as yeast.

recently shown using single-molecule fluorescence localization and super-resolution imaging of cells that CtIP and MRN localize at DSBs through interactions with each other and BRCA1 [28]. Recently, the structure of *Chaetomium thermophilum* MRN was determined using cryo-EM, and has provided new insights into the different DNA binding modes and activities of the complex [29]. The MRN complex comprises a dimer of MRE11-RAD50 and monomeric NBS1 (Xrs2 in yeast) that assemble in a unique structure with a globular ATP-dependent DNA binding and nuclease head domain and two 60 nm coiled-coils, ending in zinc-hook motifs. MRE11-RAD50 dimerization occurs via the MRE11 globular domain as well as via the zinc-hook motifs at the tip of the RAD50 coiled-coils. This particular arrangement has inspired a variety of models to account for its function in the processing and linkage of DNA [29,30]. The MRE11 subunit physically interacts with CDK2 that is required for CtIP phosphorylation and BRCA1 interaction, resulting in the recruitment of CtIP by MRN [26]. MRE11 displays both 5′–3′ endonuclease and 3′–5′ exonuclease activity, and DNA end resection occurs in a two-step manner. The CtIP-stimulated MRE11 first nicks the 5′ terminated strand at an internal position proximal to the end, then the 3′–5′ exonucleolytic activity of MRE11 removes the 5′ strand towards the break locus [7,10,27]. An intrinsic endonuclease activity of CtIP has been reported [31–33]. However, other studies did not detect significant nuclease activity for CtIP [7,34], and its putative nuclease activity requires further validation. Experiments have shown that MRN and CtIP play a role in

removing blocked ends (extensively discussed in [10]). The NHEJ factor Ku is present in the nucleus at high concentrations [35], and the HR machinery often encounters Ku-blocked DNA ends. Single-molecule experiments, in which DNA molecules are extended and exposed to fluorescently labeled Ku and MRN, indicate that Ku-blocked ends can be successfully cut by MRN alone or in complex with CtIP [36,37] (Figure 2A). Moreover, there is now evidence *in vivo* that the initial step of NHEJ involving DSB recognition by Ku-DNA-dependent protein kinase catalytic subunit (DNA-PKcs) is a target for MRN-CtIP-mediated cleavage, thereby diverting the damage response towards HR [38]. A role in DNA bridging of these protein complexes is also appealing given the particular structure of the MRN and CtIP complexes. MRN complexes can oligomerize bridging DNA molecules ~120 nm apart [29,30]. Similarly, CtIP assembles as a tetrameric dumbbell-shaped particle that can bridge DNA ends, as assessed from AFM imaging and biochemical studies [34] as well as nanofluidic assays [39]. How MRN and CtIP might combine functions in DNA bridging, and as a recruitment hub in short-range resection is not well understood.

### Long-range end resection

The main function of the short-range resection step is to remove complex DNA end structures. However, for DNA recombination a long 3′-terminated single-stranded (ss)DNA must be generated, and this is achieved by a set of helicases and nucleases working together (Figure 1B). Two routes have been reported for long-range resection. On the one hand, the EXO1 exonuclease can act alone to degrade the DNA with 5′–3′ polarity. On the other hand, Bloom syndrome helicase (BLM; Sgs1 in budding yeast) and Werner helicase (WRN) can act as a lead helicase to unwind the DNA ends, producing replication protein A (RPA)-coated ssDNA. Then, RPA directs the DNA2 helicase-nuclease to digest the 5′-terminated strand by moving on ssDNA with 5′–3′ polarity [40,41].

Although resection has been described as occurring in two different stages catalyzed by distinct factors, there is interplay between the short and long-range resection steps. DNA curtains assays have shown that MRN plays a nuclease-independent structural role in promoting track resection by recruiting EXO1 and enhancing its processivity [37]. This is consistent with biochemical assays showing that MRN promotes both the DNA2-BLM- and EXO1-mediated routes [40–42]. Furthermore, some studies support a model in which the two resection stages are coupled. In this scenario, the incision resulting from MRE11 endonuclease activity initiates the resection, followed by digestion of the 3′ to 5′ track towards the DNA end by the MRE11 exonuclease activity while the 5′ to 3′ track is digested by EXO1/BLM away from the DNA end [43]. Similarly, magnetic tweezer experiments have showed that CtIP phosphorylation strongly stimulates the motor activity of DNA2 to promote the displacement of RPA that is needed for ssDNA degradation [44]. These results are in agreement with previous biochemical work which showed that CtIP stimulates the BLM-DNA2-mediated route by enhancing the helicase activity of BLM, as well as the nuclease activity of DNA2 [45]. Moreover, experiments using single-molecule fluorescence localization and super-resolution imaging of cells showed that the nucleases EXO1 and DNA2 are recruited to the DSB site and colocalize with each other and the BLM helicase, suggesting that multiple resection strategies might occur simultaneously [28].

On a different note, compelling single-molecule imaging studies using DNA curtains have revealed that the BLM helicase forms a large transient ssDNA loop during unwinding of double-stranded (ds)DNA [46] (Figure 2B). The selection of the technique in this case is highly appropriate, as single-tethered DNA curtains enable direct visualization of fluorescently labeled protein activity on the exposed DNA ends. By labeling the 3′ ends of the DNA, the authors demonstrated that BLM helicase secures the unwound 3′-ssDNA end while translocating and unwinding the dsDNA in the presence of RPA or both DNA2 and RPA [46]. The loop might be generated either as a result of BLM maintaining a direct contact to the 3′-ssDNA end or by an interaction between BLM and RPA tethered to the ssDNA end. However, an earlier report demonstrated that BLM
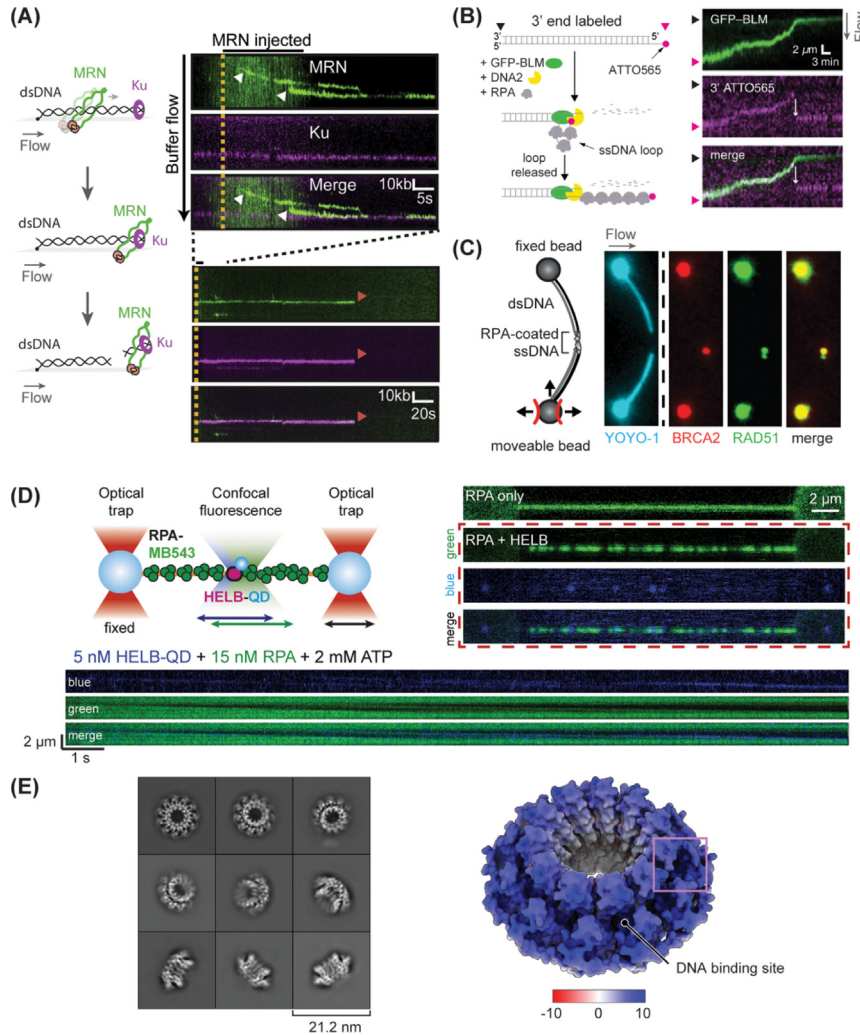
**Figure 2. Representative single-molecule studies on the homologous recombination (HR) pathway.** (A) (Left panel) Cartoon of a single DNA molecule in a DNA curtains assay where the accessible end is blocked by the Ku heterodimer. MRN binds and slides along the DNA molecule, and eventually cuts the DNA end, removing the Ku block. (Right panel) Kymograph of a single DNA molecule, displaying labeled MRN and Ku emission on the *y* axis (top position for the anchored DNA end, bottom position for accessible DNA) over time (*x* axis) (reproduced from [37]). (B) (Left panel) Cartoon of a DNA curtains assay using 3′-labeled DNA molecules. The 5′ end is accessible for processing by GFP-labeled BLM. (Right panel) Kymograph of a single DNA molecule, demonstrating looping of 3′-terminated single-stranded (ss)DNA by the BLM helicase, followed by successive loop release (adapted from [46]). (C) (Left panel) Cartoon of a double-stranded (ds)DNA–ssDNA hybrid molecule immobilized between two optically trapped beads in a setup that combines optical tweezers and fluorescence microscopy. (Right panel) The first frame displays the emission of the dsDNA-intercalating dye YOYO-1, allowing visualization of the hybrid DNA molecule. The second and third frames show the individual emissions of labeled BRCA2 and labeled RAD51, and the last frame shows the colocalization of both emissions. BRCA2 mediates the nucleation of RAD51 on RPA-covered ssDNA (adapted from [54]). (D) (Left panel) Cartoon of a dual trap optical tweezers setup in which a single DNA molecule is immobilized between two optically trapped beads, and emissions from labeled proteins are detected by confocal scanning along the DNA. (Right panel) Frames showing binding of labeled RPA and labeled HELB to the DNA. (Bottom panel) Kymographs demonstrating the movement of the proteins along the DNA and revealing that HELB removes RPA from ssDNA (adapted from [58]). (E) (Left panel) Cryo-EM projections of individual protein complexes with different orientations. (Right panel) Cryo-EM solved protein complex structure of the HR mediator RAD52 (adapted from [65]). Panels (B–E) were adapted from open access articles under CC-BY license (HYPERLINK "http://creativecommons.org/licenses/by/4.0/"http://creativecommons.org/licenses/by/4.0/). Abbreviations: Cryo-EM, cryogenic electron microscopy; MRN, MRE11-RAD50-NBS1 complex; RPA, replication protein A.

was unable to interact with RPA-coated ssDNA [47], although a stimulatory effect on dsDNA unwinding was observed with RPA free in solution [48]. ssDNA-binding proteins are known to help stabilize the nascent single strands produced by the activity of helicases, including during bacterial DNA break resection [49,50]. Thus, it is tempting to speculate that a similar effect occurs with RPA and BLM.

### Recombinase loading

The long-range resection stage results in a 3′-overhang strand covered by RPA. A complex process of replacement of RPA by recombinase RAD51, that is responsible for downstream homology search, then takes place (Figure 1C). RAD51 assembles as a helical nucleoprotein filament on ssDNA [51]. The higher binding affinity of RPA for ssDNA compared with RAD51 does not favor the formation of the RAD51 nucleoprotein filament [52] and this is facilitated by the action of positive mediators such as BRCA2 and RAD52 [53–55]. BRCA2 binds to RAD51, ssDNA, and dsDNA with different affinities, and it has been shown using AFM imaging and biochemical assays that BRCA2 catalyzes the loading of RAD51 onto RPA-covered ssDNA [56]. In a recent single-molecule assay, Bell *et al.* used optical tweezers and fluorescence to directly visualize the BRCA2-mediated nucleation of RAD51 on RPA-covered ssDNA [54] (Figure 2C). In turn, this work complements earlier studies that used similar single-molecule imaging methods to evaluate the rate of RPA displacement in the presence and absence of BRCA2 [55]. From these results it was evident that BRCA2 stimulates the replacement of RPA by RAD51 filaments. The current view is that BRCA2 assembles several RAD51 molecules through direct binding, and chaperones this small RAD51 nucleation filament to the RPA-covered ssDNA. It then loads and secures the RAD51 nucleation filament onto the ssDNA, thus stimulating the filament growth with 5′–3′ polarity [54]. In budding yeast, Rad52 is the major mediator of Rad51 loading onto RPA-covered ssDNA and plays a role analogous to that of BRCA2 [9,11]. The *Saccharomyces cerevisiae* Rad51 paralog complex Rad55–Rad57 has recently been the subject of a study using DNA curtains in which both ends of single DNA molecules are immobilized on a surface and the binding of proteins is assessed through fluorescence [57]. These proteins are positive recombination mediators that promote the nucleation of RAD51 filaments through transient interactions during the earliest stages of filament assembly. It is plausible that the action of these RAD51 filament catalysts might be coupled to the action of mediators that efficiently remove RPA from ssDNA. In support, recent experiments using fluorescence microscopy-correlated optical trapping showed that HELB, a DNA replication and HR regulatory factor, can efficiently evict RPA from ssDNA while translocating in a 5′–3′ direction (Figure 2D). The helicase activity of HELB was also measured, but it was weak in the absence of an assisting force. Additional experiments with magnetic and optical tweezers also revealed loop formation by HELB [58]. By contrast, HELB has been reported to limit long-range resection by antagonizing the processive resection nucleases EXO1 and DNA2/BLM [59]. Together these results might suggest that the presence of RPA is important for resection processivity.

By contrast, negative recombination mediator proteins disrupt RAD51-ssDNA filament formation as a regulatory mechanism to moderate the action of RAD51. Recent studies using single-molecule assays have revealed that RADX condenses ssDNA and antagonizes RAD51 functions by disturbing the RAD51 nucleofilament [60,61]. Employing a DNA curtains assay, Adolph *et al.* found that, with increasing concentrations of RADX, RAD51 assembly on RPA-covered ssDNA diminishes as RADX competes for ssDNA binding [60]. Moreover, a RAD51 ATPase assay showed that RADX induces ATP hydrolysis by ssDNA-bound RAD51, which leads to nucleofilament destabilization. An alternative mechanism for disturbing the formation of the RAD51 nucleoprotein filament was proposed by Zhang *et al.* [61]. Using DNA curtains, the authors demonstrated that RADX condenses RPA-covered ssDNA, which in turn prevents RPA displacement and inhibits RAD51 binding [61]. The yeast helicase Srs2 is another example of a negative regulator, or anti-recombinase, that efficiently removes the RAD51 filament from

ssDNA. In DNA curtains experiments, Srs2 was seen translocating along RAD51-covered ssDNA, thus removing RAD51 and allowing RPA loading onto the newly exposed ssDNA [62]. Similar single-molecule experiments also demonstrated that Srs2 is a powerful helicase that can remove other ssDNA binding proteins such as RPA and RAD52 while translocating [63].

### Strand invasion and homology search

Finally, the nucleoprotein filament of RAD51 initiates downstream strand invasion and homology search, which facilitates template-based DNA synthesis driven by polymerases (Figure 1D). The homology search by RAD51 has been addressed by Brouwer *et al.* in a combined single-molecule confocal-optical tweezers and X-ray crystallography study that described how RAD51 can exist in two interconvertible ATP-dependent conformational states [64]. RAD54 and RAD52 are major factors involved in this strand-invasion stage. RAD52 promotes the annealing of complementary DNA, and *in vitro* experiments have shown that human RAD52 can catalyze the formation of D-loops [11,13]. The cryo-EM structure of full-length human RAD52, at an average resolution of 3.5 Å, has been recently published and reveals more details of an intrinsically complex assembly [65] (Figure 2E). RAD54 is an ATP-dependent protein motor with DNA translocation, DNA supercoiling, and chromatin remodeling activities. RAD54 interacts with RAD51 at several stages from promoting homology search to facilitating D-loop formation and dissolving the D-loop upon completion of DNA synthesis [13,66,67].

In contrast to the multiple single-molecule studies that address different aspects of DSB recognition and end processing, few have addressed homology search and recombination. This probably reflects the difficulty of manipulating several DNA molecules simultaneously. A few single-molecule studies using bacterial recombinase RecA have been reported [68–70]. A manipulation system combining magnetic and optical tweezers enabled the manipulation of two molecules simultaneously. The molecules could be locally contacted, allowing protein-mediated DNA binding. The strength of these interactions could then be investigated by pulling the molecules apart [68]. Another study using magnetic tweezers and complex DNA substrates with hairpins showed that strand invasion is blocked by homology mismatches [69]. Recently, in a study using smFRET, the authors were able to resolve the donor strand-separation step from base-pair formation [70]. An elegant recent report described the contribution of human HELQ to the annealing of complementary DNA [71]. In this work, single-molecule assays using combined optical trapping and fluorescence microscopy showed that DNA unwinding by HELQ is strongly stimulated by RAD51, whereas RPA promoted strand annealing of labeled oligonucleotides to RPA-covered ssDNA [71].

Once the strand invasion and homology search steps are completed, the invading strand undergoes elongation via HR polymerases that mediate template-driven synthesis from the 3′ end. At this point the HR pathway follows two main subpathways: double Holliday junction (dHJ) and synthesis-dependent single-strand annealing (SDSA) (reviewed in detail in [72,73]). Few single-molecule studies have addressed the reactions of these subpathways. However, a recent single-molecule study using optical tweezers and confocal microscopy investigated the processing of Holliday junctions by junction-resolving enzymes [74]. As single-molecule assays become more sophisticated and combine several techniques, addressing the intermediate steps of these complex intermolecular reactions will become increasingly feasible, and we expect to see an increase of reported findings.

### Non-homologous end joining
#### DSB detection and initiation of the NHEJ pathway

NHEJ is the predominant pathway for DSB repair in humans [75]. This dynamic pathway involves a multitude of proteins which recognize the break, bridge and process the two free ends, and

finally ligate them (Figure 3 and Table 2). Understanding the dynamics of the NHEJ supercomplexes and how they cooperate or are modulated by additional factors is a subject of intensive research. Upon formation of a DSB, 53BP1 is recruited to the damaged chromatin. 53BP1 is an important positive regulator of the NHEJ pathway that accumulates as a response to ATM activation. It promotes NHEJ throughout the cell cycle, and during the G1 phase it protects DSB ends from resection by the HR machinery [14,23,24].
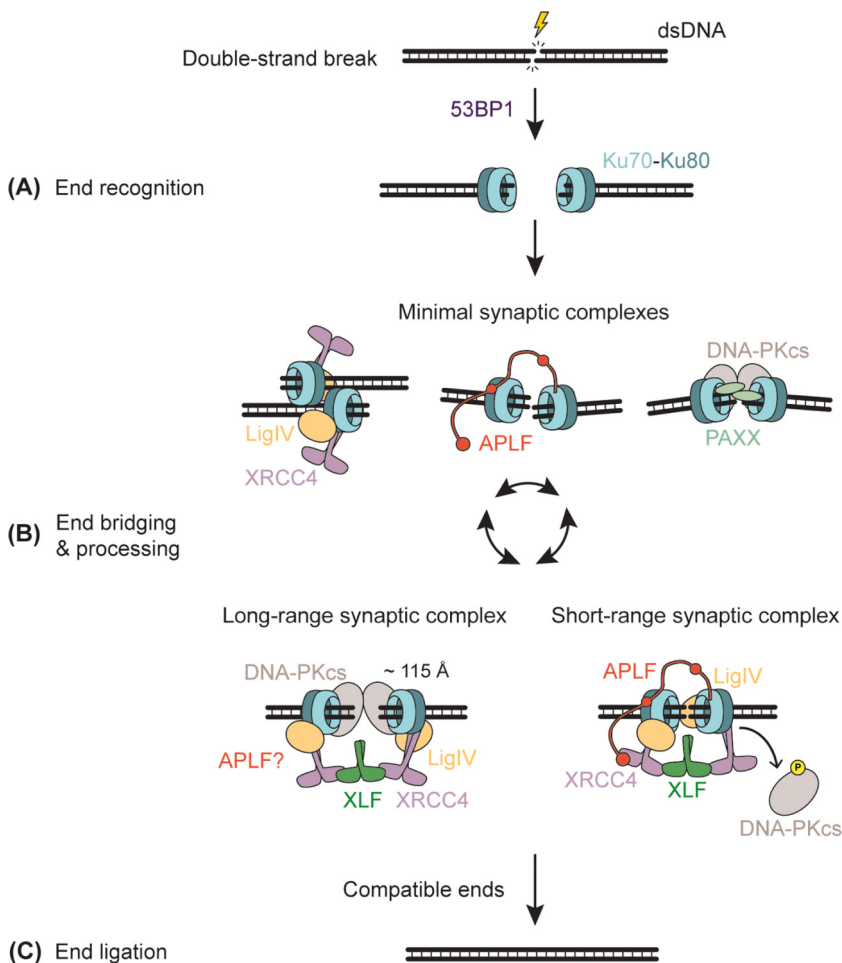


Figure 3. Cartoon of the current view on the non-homologous end joining (NHEJ) pathway. (A) End recognition. The NHEJ repair pathway initiates with the accumulation of 53BP1 at the damaged chromatin followed by recognition of the DNA ends by the Ku heterodimer This pathway is an interactive and dynamic process which promotes the fastest repair possible while minimizing mutagenesis. (B) End bridging and processing. Several minimal synaptic complexes have been described. These minimal complexes position the two DNA ends in close proximity, probably to immobilize to some extent the break site while the core NHEJ factors are being recruited. NHEJ supercomplexes are composed of a multitude of factors with structural and catalytic roles. NHEJ accessory factors include nucleases, polymerases, and damage-correction enzymes that can process the DNA ends. Two major synaptic configurations have been defined: the long- and the short-range synaptic configurations. The former is composed of all core NHEJ factors and the DNA ends are kept 115 Å apart. The latter contains all core factors except for DNA-PKcs, and the DNA ends are aligned and ready for ligation as soon as the DNA ends are compatible. (C) End ligation. DNA ligase IV (LigIV) seals the nicks at both strands, thus completing the repair of the double-strand break. Abbreviations: DNA-PKcs, DNA-dependent protein kinase catalytic subunit; dsDNA, double-stranded DNA; P, phosphorylation; XRCC4, X-ray repair cross complementing 4; XLF, XRCC4-like factor.

Table 2. NHEJ factors addressed in this review[a]

| Eukaryotic* | Function | Refs |
|---|---|---|
| 53BP1 | NHEJ promoter | [14,23–25] |
| Ku70–Ku80 (Ku) | DSB recognition Recruitment of the repair hub | [2,35–38,76,77,80–89,97] |
| DNA-PKcs | Kinase activity Structural role in synapsis End-processing mediator | [38,76,77,80,83–90] |
| XRCC4 | Structural role Ku, XLF, and LigIV interactor | [78–80,82–88,92–94] |
| XLF | XRCC4 and Ku interactor Structural role in synapsis | [64,78,80–88,93,94] |
| DNA ligase IV (LigIV) | Catalytic role in ligation Structural role in synapsis | [83–85,87,88,99–101] |
| APLF | Structural role in synapsis Scaffolding role | [84] |
| PAXX | Structural role in synapsis | [82,83] |

[a]All the proteins listed are human.

## DNA end recognition and repair hub recruitment

The first NHEJ core factor to arrive at the DSB is the Ku70/Ku80 heterodimer (Ku) that binds to dsDNA ends with high affinity (Figure 3A). Ku assembles as a ring that threads onto the DSB ends with Ku70 subunit facing the free end [35]. Ku offers protection against the action of nucleases and acts as a recruiting hub for the rest of the core factors responsible for end bridging and processing [2].

Next, a set of core proteins including DNA-PKcs, X-ray repair cross complementing 4 (XRCC4), XRCC4-like factor (XLF), and DNA ligase IV (LigIV) assemble around the Ku-bound DNA ends, constituting a repair hub whose mission is to keep the two DNA ends joined while attempting to generate compatible DNA ends for ligation. DNA-PKcs is a recent evolutionary addition to NHEJ, as yeast lacks this protein. It forms a complex with Ku and DNA and has been described to interact with several accessory factors to offer structural support to the bridged DNA ends while also making them accessible for processing [76,77]. XRCC4 and XLF share structural similarities: both harbor a globular head domain followed by an elongated α-helical stalk, a disordered C-terminal region, and assemble as dimers [78,79]. The flexible C-terminal tail of XLF contains a Ku-binding motif (X-KBM) that anchors XLF to Ku-DNA and allows it to scavenge for interactions within the synaptic complex [80,81] The N terminal coiled-coil stalks of XRCC4 form a constitutive complex with LigIV. This complex is responsible for the covalent ligation of the DNA ends and offers structural support to the synaptic complex [79].

## DNA end bridging and processing

Several works have reported different minimal combinations of proteins that support end bridging (Figure 3B). In smFRET experiments with purified Ku, XRCC4-LigIV, and XLF, Zhao *et al.* reported that Ku and XRCC4-LigIV are sufficient to obtain a flexible lateral bridging of DNA ends and that the further addition of XLF or PAXX, an accessory factor, drives the dsDNA ends into an end-to-end configuration [82]. The smFRET configuration used in this study is well suited for the biology investigated, as two accessible DNA ends are required for a single end-bridging event. Moreover, the distance-dependent intensity of the FRET signal provides valuable insights into the composition of the bridging complex formed. Employing a compelling magnetic tweezers assay, in which a DSB is mimicked, and the bridging of DNA ends is detected as a reduction in DNA extension,

Wang *et al.* revealed that PAXX makes a structural contribution to the synapsis of DNA ends. PAXX robustly stabilizes the bridge mediated by Ku and DNA-PKcs, and further supports the synapsis mediated by all the core factors, Ku-DNA-PKcs-XRCC4-LigIV-XLF [83]. Recently, a further study using a similar approach revealed the ability of APLF, another accessory factor, to bridge Ku-bound DNA ends and maintain the synapsis for several minutes under applied forces of 2 pN [84] (Figure 4A). A scavenger role for APLF in searching for Ku-bound DNA ends was proposed in addition to its previously defined scaffolding role. Both PAXX and APLF had been considered accessory factors, but their contributions to end bridging, which had been obscured by the other core factors, have now been unveiled using single-molecule methods.

The core NHEJ proteins form supercomplexes (Figure 3B). In Graham *et al.* the synapsis of DNA ends by *Xenopus laevis* egg extracts was studied by combining single-molecule colocalization fluorescence microscopy and smFRET. This work suggested the coexistence of two conformational states in end synapsis that consist of either long-range or short-range complexes [85] (Figure 4B). In the long-range configuration, the bridged DNA ends are visualized by colocalization fluorescence, but the donor and the acceptor dyes are too far apart to induce FRET. By contrast, in the short-range configuration, FRET is detected between the dyes, indicating a close configuration. The conversion from the long-range to the short-range configuration required the presence of XLF, XRCC4, and LigIV, as well as the catalytic activity of DNA-PKcs [85]. A follow-up study using smFRET revealed that the bridging of DNA ends in the short-range configuration is mediated by a single XLF dimer [80]. Using the same smFRET technique, Carney *et al.* demonstrated that the XLF C-terminal tail is necessary to form the short-range complex [86]. It was proposed that the Ku-binding motif in XLF is responsible for linking XLF to Ku while the flexibility of the XLF C-terminal tail scavenges for interactions with XRCC4 [86]. Structural studies by Chen *et al.* using single-particle cryo-EM reported the structure of the long-range synaptic complex. The two ends of the DNA break are bridged by a protein scaffold consisting of LigIV-XRCC4-XLF-XRCC4-LigIV and the intermolecular interactions between the DNA-PK catalytic subunits. The DNA ends in this configuration are kept ~115 Å apart [87]. Chen *et al.* also reported the structure of the short-range synaptic complex composed of the same protein scaffold, LigIV-XRCC4-XLF-XRCC4-LigIV, that binds to both Ku-bound ends, but DNA-PKcs is absent. This XLF-mediated synaptic structure confirmed that a single dimer of XLF supports the bridging. Interestingly, the absence of DNA-PKcs in the short-range synaptic complex suggested that the transition to the short-range configuration requires DNA-PKcs autophosphorylation in *trans* and its subsequent release from the DNA ends [87]. A contemporaneous publication by Chaplin *et al.* [88] validated the configuration of the long-range synaptic complex reported by Chen *et al.* [87] (Figure 4C). In previous work they reported an alternative long-range synaptic complex consisting of only Ku and DNA-PKcs [89]. In this alternative supercomplex, the synapsis of the DNA ends is mediated by a domain swap of the Ku80 subunits on both sides of the break. Interestingly, the DNA ends in this complex are also ~115 Å apart. However, this alternative configuration would not seem to facilitate ligation. Using cellular models, this alternative long-range complex has recently been associated with specific types of DNA-end chemistry [90].

In contrast to the HR pathway, NHEJ prioritizes end ligation over end processing [2], and as soon as the DNA ends are compatible for ligation, LigIV seals the nicks on both strands, thus repairing the break. However, broken ends are not always compatible with direct ligation, and minimal processing of DNA ends might be required. This includes the activity of end-processing enzymes such as nucleases and polymerases which modify DNA ends to prepare them for ligation [2]. Interestingly, FRET experiments show that the processing of the DNA ends occurs preferentially in the short-range configuration, possibly to ensure that the DNA ends undergo ligation as soon as they become compatible [91]. In agreement with these single-molecule experiments, Chen *et al.*
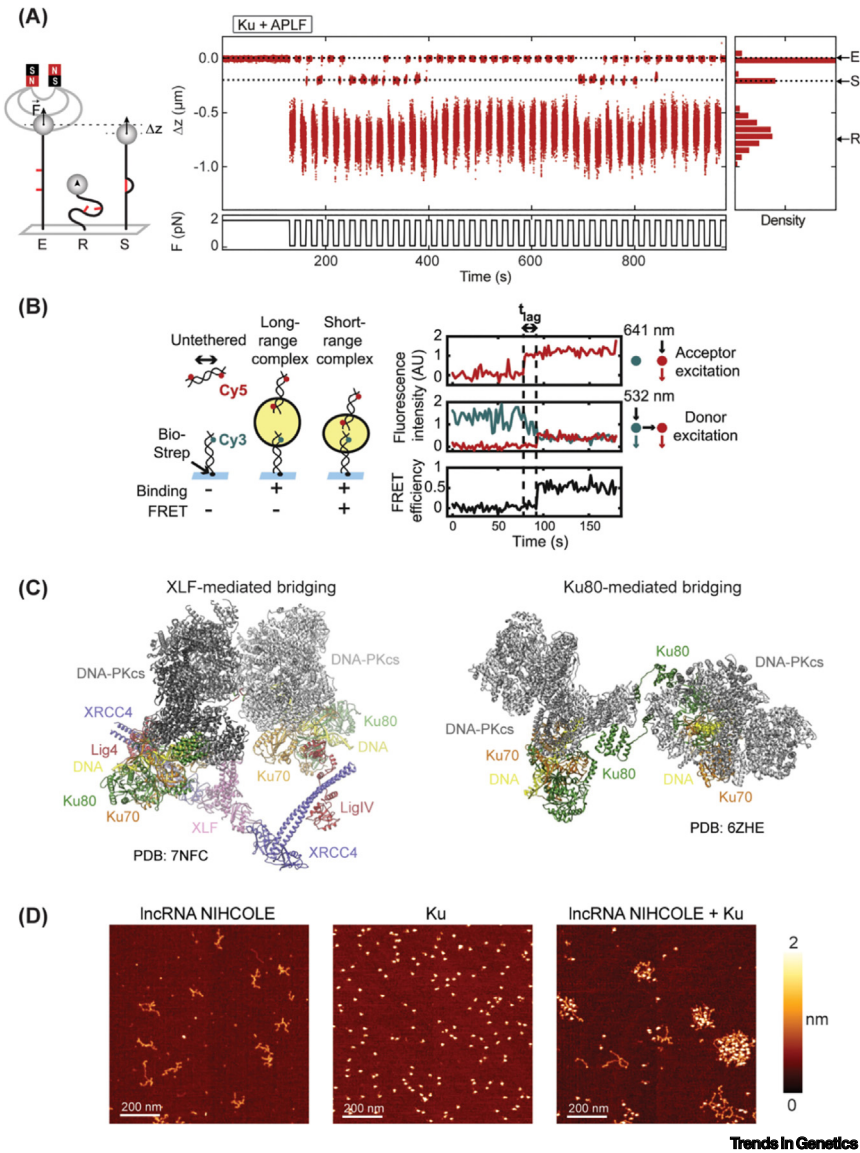
**Figure 4. Representative single-molecule studies on the non-homologous end joining (NHEJ) pathway.** (A) (Left panel) Cartoon of a single DNA molecule tethered to a glass surface and connected to a magnetic bead within a magnetic tweezers setup. Applying magnetic force to the bead extends the DNA molecule 'E'. Releasing the force allows the DNA to relax 'R'. This unique molecule has two DNA branches that proteins in the solution can bridge when the DNA is relaxed. Applying tension to the bridged DNA leads to an apparent reduction in DNA extension in a synaptic state 'S'. (Right panel) Timecourse of a DNA molecule being alternately relaxed and stretched in the presence of Ku and APLF, illustrating end-bridging facilitated by these two proteins (reprinted, with permission, from [84]). (B) (Left panel) Cartoon depicting a fluorescence resonance energy transfer (FRET) assay in which a Cy3-labeled DNA molecule is tethered to a surface, and untethered Cy5-labeled DNA molecules are present in solution. When proteins capable of bridging DNA are introduced, the two DNA molecules can be joined. (Right panel) By exciting the separate fluorophores, their colocalization becomes possible. In a specific close configuration, excitation of the Cy3 fluorophore results in Cy5 fluorophore emission as a result of energy transfer between them. The two distinct synaptic configurations, short- and long-range, were first identified in FRET experiments (reprinted, with permission, from [85]). (C) (Left panel) Cryo-electron microscopy (cryo-EM) resolved XRCC4-like factor (XLF)-mediated synaptic complex bridging two DNA ends. (Right panel) Cryo-EM reconstruction of the Ku80-mediated DNA end bridging (adapted, with permission, from [88]). (D) Atomic force microscopy (AFM) imaging shows localized collection of long noncoding (lnc)RNA *NIHCOLE* promoted by the Ku heterodimer (adapted, with permission, from [97]). Abbreviations: DNA-PKcs, DNA-dependent protein kinase catalytic subunit; PDB, Protein Data Base; XRCC4, X-ray repair cross complementing 4.

showed that the transition to the short-range configuration aligns the Ku-bound ends to enable processing and ligation [87].

It is now well established that the step of end bridging and processing involves supercomplexes working cooperatively. Nevertheless, there are still many open questions related to recent discoveries. Filaments of XRCC4 and XLF have been described *in vitro* and visualized by single-molecule assays [92–94], but the relevance of these filaments to DNA repair is unclear. Using dual-trap and quadrupole-trap optical tweezers combined with fluorescence microscopy, Brouwer *et al.* showed that both XRCC4 and XLF transiently bind and diffuse along dsDNA, and that XRCC4 binding to DNA is stimulated by XLF [92]. Another interesting line of research involves noncoding (nc)RNAs. Several ncRNAs have been associated with NHEJ [95–98]. *LINP1*, a long noncoding RNA (lncRNA) that is overexpressed in breast cancer, was shown in magnetic tweezers experiments to increase the lifetime of synaptic complexes [96]. Similarly, a recent study also using magnetic tweezers showed that lncRNA *NIHCOLE*, an RNA overexpressed in hepatocellular carcinoma cells, fortifies the synaptic complex [84]. The interaction of *NIHCOLE* and Ku was visualized by AFM imaging (Figure 4D), and *NIHCOLE* has been defined as a mediator that promotes the efficiency of the ligation by LigIV, as observed in *in vitro* assays [97]. The selection of the single-molecule approach in this instance is notably fitting as AFM imaging enables the direct observation of biological complexes without the need for manipulation that might inadvertently disturb their intricate structure.

### DNA end ligation

The final stage of the NHEJ pathway is the ligation of the two nicks, one on each strand of the DSB (Figure 3C). This is performed by two LigIV molecules present in the short-range supercomplex, each dealing with one nick [87]. Several single-molecule studies have addressed the impact of diverse end structures on the catalysis of end-ligation by LigIV [99–101]. Recently, smFRET studies showed that a mutation in the LigIV DNA-binding domain blocks the conversion from the long- to the short-range configuration, which indicates that the presence of the LigIV near the DSB break is imperative for the short-range processing of DNA ends. Additional experiments also showed that a single LigIV can bind to both DNA ends at the same time in the closest configuration [101].

### Concluding remarks and future directions

Single-molecule assays are becoming more sophisticated and continue to push technological and experimental boundaries by combining several techniques. The most versatile methods combine manipulation and visualization. Single-molecule methods are unique in that they offer the possibility to manipulate individual DNA molecules and to engineer constructs that mimic repair intermediates. Importantly, they also allow one to probe the interaction with proteins. Moreover, direct visualization provides mechanistic insights and access to dynamic information such as diffusion rates, motor protein translocation and unwinding rates, directionality, dwell times, pause kinetics, stall forces, and so forth. In turn, creativity plays an important role in the design and development of new single-molecule assays to address cryptic questions in DNA repair. This involves not only technical improvements to the setups but also the construction of increasingly complex DNA structures. Some DNA configurations of particular biological interest include those containing DNA ends, ss–dsDNA interfaces, and D-loop and Holliday junction structures, among others. DNA nanotechnology can also potentially solve some of the structural challenges in the development of new single-molecule assays. For example, DNA origami structures composed of two perfectly aligned equivalent molecules, that are sufficiently close to allow strand invasion and homology search in the presence of the appropriate machinery, could reveal how the damaged strand interacts with the donor strand in the HR pathway.

### Outstanding questions

What molecular mechanisms are involved in preventing the separation of the two DNA ends to ensure precise repair by HR?

Do short-range and long-range resection events occur concurrently during HR?

What specific molecular mechanisms are responsible for the homology search of the damaged DNA within the sister chromatid during HR?

What are the mechanisms by which lncRNAs regulate the repair process through the NHEJ pathway?

Are DNA repair reactions a series of independent sequential steps or a series of linked DNA transactions that are orchestrated by dynamically interacting proteins?

Is it possible to reproduce at the single-molecule level the entire DSB repair pathways from purified components?

Although considerable progress has been made in the production of diverse DNA structures for single-molecule experiments, new experimental challenges continually arise, including the need to make the assays more efficient and high-throughput. AFM is a high-throughput technique and could in principle solve this problem. However, AFM cannot distinguish between two different proteins of similar topology or protein components within a complex. The combination of AFM with super-resolution fluorescence methods might help to overcome this challenge as one could identify a particular labeled protein from the AFM image. The ultimate combination of fast AFM imaging with super-resolution fluorescence could be insightful for investigating, for instance, whether short-range and long-range resection events occur concurrently during HR by directly observing the activity of MRN and/or EXO1/DNA2-BLM. A similar approach could be envisaged to investigate the iterative nature of the DNA repair machinery in NHEJ. Overall, the combination of single-molecule manipulation techniques with super-resolution fluorescence microscopy represents a very interesting developing route to increase spatial resolution. However, this improvement will come at the expense of time resolution, a factor that might be essential in some processes involving molecular motors.

We believe that in the coming years we will witness the development of new assays designed to specifically address outstanding questions in the field, such as the homology search and strand invasion steps in HR, or the interplay between the different components of the NHEJ machinery (see Outstanding questions). These new assays will involve the construction of more sophisticated instruments with improved spatial and temporal resolution, as well as high-throughput data acquisition and analysis.

## Declaration of interests

The authors declare no competing interests

## References

1. Cejka, P. and Symington, L.S. (2021) DNA end resection: mechanism and control. *Annu. Rev. Genet.* 55, 285–307
2. Stinson, B.M. and Loparo, J.J. (2021) Repair of DNA double-strand breaks by the nonhomologous end joining pathway. *Annu. Rev. Biochem.* 90, 137–164
3. Alhmoud, J.F. *et al.* (2020) DNA damage/repair management in cancers. *Cancers* 12, 1050
4. Mao, Z. *et al.* (2008) Comparison of nonhomologous end joining and homologous recombination in human cells. *DNA Repair* 7, 1765–1771
5. Kong, M. and Greene, E.C. (2021) Mechanistic insights from single-molecule studies of repair of double strand breaks. *Front. Cell Dev. Biol.* 9, 745311
6. Ranjha, L. *et al.* (2018) Main steps in DNA double-strand break repair: an introduction to homologous recombination and related processes. *Chromosoma* 127, 187–214
7. Andres, S.N. and Williams, R.S. (2017) CtIP/Ctp1/Sae2, molecular form fit for function. *DNA Repair* 56, 109–117
8. Chaplin, A.K. and Blundell, T.L. (2020) Structural biology of multicomponent assemblies in DNA double-strand-break repair through non-homologous end joining. *Curr. Opin. Struct. Biol.* 61, 9–16
9. Morati, F. and Modesti, M. (2021) Insights into the control of RAD51 nucleoprotein filament dynamics from single-molecule studies. *Curr. Opin. Genet. Dev.* 71, 182–187
10. Reginato, G. and Cejka, P. (2020) The MRE11 complex: a versatile toolkit for the repair of broken DNA. *DNA Repair* 91–92, 102869
11. Rossi, M.J. *et al.* (2021) RAD52: paradigm of synthetic lethality and new developments. *Front. Genet.* 12, 780293
12. Roy, U. and Greene, E.C. (2021) The role of the Rad55–Rad57 complex in DNA repair. *Genes* 12, 1390
13. San Filippo, J. *et al.* (2008) Mechanism of eukaryotic homologous recombination. *Annu. Rev. Biochem.* 77, 229–257
14. Shibata, A. and Jeggo, P.A. (2021) ATM's role in the repair of DNA double-strand breaks. *Genes* 12, 1370
15. Watanabe, G. and Lieber, M.R. (2022) Dynamics of the Artemis and DNA-PKcs complex in the repair of double-strand breaks. *J. Mol. Biol.* 434, 167858
16. Kang, Y. *et al.* (2022) Single-molecule fluorescence imaging techniques reveal molecular mechanisms underlying deoxyribonucleic acid damage repair. *Front. Bioeng. Biotechnol.* 10, 973314
17. Kaniecki, K. *et al.* (2018) A change of view: homologous recombination at single-molecule resolution. *Nat. Rev. Genet.* 19, 191–207
18. Xu, L. *et al.* (2023) Unravelling how single-stranded DNA binding protein coordinates DNA metabolism using single-molecule approaches. *IJMS* 24, 2806
19. Liang, S. *et al.* (2021) Stages, scaffolds and strings in the spatial organisation of non-homologous end joining: insights from X-ray diffraction and cryo-EM. *Prog. Biophys. Mol. Biol.* 163, 60–73

20. Watanabe, G. and Lieber, M.R. (2023) The flexible and iterative steps within the NHEJ pathway. *Prog. Biophys. Mol. Biol.* 180, 105–119

21. Shibata, A. *et al.* (2011) Factors determining DNA double-strand break repair pathway choice in G2 phase: DSB repair pathway choice in G2 phase. *EMBO J.* 30, 1079–1092

22. Jansma, M. and Hopfner, K.-P. (2021) Structural basis of the (in)activity of the apical DNA damage response kinases ATM, ATR and DNA-PKcs. *Prog. Biophys. Mol. Biol.* 163, 120–129

23. Panier, S. and Boulton, S.J. (2013) Double-strand break repair: 53BP1 comes into focus. *Nat. Rev. Mol. Cell Biol.* 15, 7–18

24. Scully, R. *et al.* (2019) DNA double-strand break repair-pathway choice in somatic mammalian cells. *Nat. Rev. Mol. Cell Biol.* 20, 698–714

25. Dai, L. *et al.* (2021) Structural insight into BRCA1–BARD1 complex recruitment to damaged chromatin. *Mol. Cell* 81, 2765–2777

26. Buis, J. *et al.* (2012) Mre11 regulates CtIP-dependent double-strand break repair by interaction with CDK2. *Nat. Struct. Mol. Biol.* 19, 246–252

27. Cannavo, E. and Cejka, P. (2014) Sae2 promotes dsDNA endonuclease activity within Mre11–Rad50–Xrs2 to resect DNA breaks. *Nature* 514, 122–125

28. Whelan, D.R. and Rothenberg, E. (2021) Super-resolution mapping of cellular double-strand break resection complexes during homologous recombination. *Proc. Natl. Acad. Sci. U. S. A.* 118, e2021963118

29. Rotheneder, M. *et al.* (2023) Cryo-EM structure of the Mre11–Rad50–Nbs1 complex reveals the molecular mechanism of scaffolding functions. *Mol. Cell* 83, 167–185

30. Kissling, V.M. *et al.* (2022) Mre11-Rad50 oligomerization promotes DNA double-strand break repair. *Nat. Commun.* 13, 2374

31. Lengsfeld, B.M. *et al.* (2007) Sae2 is an endonuclease that processes hairpin DNA cooperatively with the Mre11/Rad50/Xrs2 complex. *Mol. Cell* 28, 638–651

32. Makharashvili, N. *et al.* (2014) Catalytic and noncatalytic roles of the CtIP endonuclease in double-strand break end resection. *Mol. Cell* 54, 1022–1033

33. Wang, H. *et al.* (2014) CtIP maintains stability at common fragile sites and inverted repeats by end resection-independent endonuclease activity. *Mol. Cell* 54, 1012–1021

34. Wilkinson, O.J. *et al.* (2019) CtIP forms a tetrameric dumbbell-shaped particle which bridges complex DNA end structures for double-strand break repair. *eLife* 8, e42129

35. Walker, J.R. *et al.* (2001) Structure of the Ku heterodimer bound to DNA and its implications for double-strand break repair. *Nature* 412, 607–614

36. Deshpande, R.A. *et al.* (2020) DNA-dependent protein kinase promotes DNA end processing by MRN and CtIP. *Sci. Adv.* 6, eaay0922

37. Myler, L.R. *et al.* (2017) Single-molecule imaging reveals how Mre11-Rad50-Nbs1 initiates DNA break repair. *Mol. Cell* 67, 891–898

38. Deshpande, R.A. *et al.* (2023) Genome-wide analysis of DNA-PK-bound MRN cleavage products supports a sequential model of DSB repair pathway choice. *Nat. Commun.* 14, 5759

39. Öz, R. *et al.* (2020) Phosphorylated CtIP bridges DNA to promote annealing of broken ends. *Proc. Natl. Acad. Sci. U. S. A.* 117, 21403–21412

40. Nimonkar, A.V. *et al.* (2011) BLM–DNA2–RPA–MRN and EXO1–BLM–RPA–MRN constitute two DNA end resection machineries for human DNA break repair. *Genes Dev.* 25, 350–362

41. Niu, H. *et al.* (2010) Mechanism of the ATP-dependent DNA end-resection machinery from *Saccharomyces cerevisiae*. *Nature* 467, 108–111

42. Shim, E.Y. *et al.* (2010) *Saccharomyces cerevisiae* Mre11/Rad50/Xrs2 and Ku proteins regulate association of Exo1 and Dna2 with DNA breaks. *EMBO J.* 29, 3370–3380

43. Shibata, A. *et al.* (2014) DNA double-strand break repair pathway choice is directed by distinct MRE11 nuclease activities. *Mol. Cell* 53, 7–18

44. Ceppi, I. *et al.* (2020) CtIP promotes the motor activity of DNA2 to accelerate long-range DNA end resection. *Proc. Natl. Acad. Sci. U. S. A.* 117, 8859–8869

45. Daley, J.M. *et al.* (2017) Enhancement of BLM–DNA2-mediated long-range DNA end resection by CtIP. *Cell Rep.* 21, 324–332

46. Xue, C. *et al.* (2022) Bloom helicase mediates formation of large single-stranded DNA loops during DNA end processing. *Nat. Commun.* 13, 2248

47. Xue, C. *et al.* (2019) Single-molecule visualization of human BLM helicase as it acts upon double- and single-stranded DNA substrates. *Nucleic Acids Res.* 47, 11225–11237

48. Qin, Z. *et al.* (2020) Human RPA activates BLM's bidirectional DNA unwinding from a nick. *eLife* 9, e54098

49. Carrasco, C. *et al.* (2013) On the mechanism of recombination hotspot scanning during double-stranded DNA break resection. *Proc. Natl. Acad. Sci. U. S. A.* 110

50. Gilhooly, N.S. *et al.* (2013) Superfamily 1 helicases. *Front. Biosci.* S5, 206–216

51. Short, J.M. *et al.* (2016) High-resolution structure of the presynaptic RAD51 filament on single-stranded DNA by electron cryo-microscopy. *Nucleic Acids Res.* 44, 9017–9030

52. Ma, C.J. *et al.* (2017) Protein dynamics of human RPA and RAD51 on ssDNA during assembly and disassembly of the RAD51 filament. *Nucleic Acids Res.* 45, 749–761

53. Ma, C.J. *et al.* (2017) Human RAD52 interactions with replication protein A and the RAD51 presynaptic complex. *J. Biol. Chem.* 292, 11702–11713

54. Bell, J.C. *et al.* (2023) BRCA2 chaperones RAD51 to single molecules of RPA-coated ssDNA. *Proc. Natl. Acad. Sci. U. S. A.* 120, e2221971120

55. Belan, O. *et al.* (2021) Single-molecule analysis reveals cooperative stimulation of Rad51 filament nucleation and growth by mediator proteins. *Mol. Cell* 81, 1058–1073

56. Sidhu, A. *et al.* (2020) Conformational flexibility and oligomerization of BRCA2 regions induced by RAD51 interaction. *Nucleic Acids Res.* 48, 9649–9659

57. Roy, U. *et al.* (2021) The Rad51 paralog complex Rad55–Rad57 acts as a molecular chaperone during homologous recombination. *Mol. Cell* 81, 1043–1057

58. Hormeno, S. *et al.* (2022) Human HELB is a processive motor protein that catalyzes RPA clearance from single-stranded DNA. *Proc. Natl. Acad. Sci. U. S. A.* 119, e2112376119

59. Tkáč, J. *et al.* (2016) HELB is a feedback inhibitor of DNA end resection. *Mol. Cell* 61, 405–418

60. Adolph, M.B. *et al.* (2021) RADX controls RAD51 filament dynamics to regulate replication fork stability. *Mol. Cell* 81, 1074–1083

61. Zhang, H. *et al.* (2020) RADX condenses single-stranded DNA to antagonize RAD51 loading. *Nucleic Acids Res.* 48, 7834–7843

62. Kaniecki, K. *et al.* (2017) Dissociation of Rad51 presynaptic complexes and heteroduplex DNA joints by tandem assemblies of Srs2. *Cell Rep.* 21, 3166–3177

63. De Tullio, L. *et al.* (2017) Yeast Srs2 helicase promotes redistribution of single-stranded DNA-bound RPA and Rad52 in homologous recombination regulation. *Cell Rep.* 21, 570–577

64. Brouwer, I. *et al.* (2018) Two distinct conformational states define the interaction of human RAD51–ATP with single-stranded DNA. *EMBO J.* 37, e98162

65. Kinoshita, C. *et al.* (2023) The cryo-EM structure of full-length RAD52 protein contains an undecameric ring. *FEBS Open Bio* 13, 408–418

66. Crickard, J.B. *et al.* (2020) Rad54 and Rdh54 occupy spatially and functionally distinct sites within the Rad51-ssDNA presynaptic complex. *EMBO J.* 39, e105705

67. Crickard, J.B. *et al.* (2020) Rad54 drives ATP hydrolysis-dependent dna sequence alignment during homologous recombination. *Cell* 181, 1380–1394

68. De Vlaminck, I. *et al.* (2012) Mechanism of homology recognition in DNA recombination from dual-molecule experiments. *Mol. Cell* 46, 616–624

69. Huang, X. *et al.* (2020) Mismatch sensing by nucleofilament deciphers mechanism of RecA-mediated homologous recombination. *Proc. Natl. Acad. Sci. U. S. A.* 117, 20549–20554

70. Yu, F. *et al.* (2023) Flanking strand separation activity of RecA nucleoprotein filaments in DNA strand exchange reactions. *Nucleic Acids Res.* 51, 2270–2283

71. Anand, R. *et al.* (2022) HELQ is a dual-function DSB repair enzyme modulated by RPA and RAD51. *Nature* 601, 268–273

72. Elbakry, A. and Löbrich, M. (2021) Homologous recombination subpathways: a tangle to resolve. *Front. Genet.* 12, 723847
73. Wright, W.D. *et al.* (2018) Homologous recombination and the repair of DNA double-strand breaks. *J. Biol. Chem.* 293, 10524–10535
74. Kaczmarczyk, A.P. *et al.* (2022) Search and processing of Holliday junctions within long DNA by junction-resolving enzymes. *Nat. Commun.* 13, 5921
75. Karanam, K. *et al.* (2012) Quantitative live cell imaging reveals a gradual shift between DNA repair mechanisms and a maximal use of HR in mid S phase. *Mol. Cell* 47, 320–329
76. Liu, L. *et al.* (2022) Autophosphorylation transforms DNA-PK from protecting to processing DNA ends. *Mol. Cell* 82, 177–189
77. Watanabe, G. *et al.* (2022) Structural analysis of the basal state of the Artemis:DNA-PKcs complex. *Nucleic Acids Res.* 50, 7697–7720
78. Andres, S.N. *et al.* (2007) Crystal structure of human XLF: a twist in nonhomologous DNA end-joining. *Mol. Cell* 28, 1093–1101
79. Sibanda, B.L. *et al.* (2001) Crystal structure of an Xrcc4–DNA ligase IV complex. *Nat. Struct. Biol.* 8, 1015–1019
80. Graham, T.G.W. *et al.* (2018) A single XLF dimer bridges DNA ends during nonhomologous end joining. *Nat. Struct. Mol. Biol.* 25, 877–884
81. Nemoz, C. *et al.* (2018) XLF and APLF bind Ku80 at two remote sites to ensure DNA repair by non-homologous end joining. *Nat. Struct. Mol. Biol.* 25, 971–980
82. Zhao, B. *et al.* (2019) The essential elements for the noncovalent association of two DNA ends during NHEJ synapsis. *Nat. Commun.* 10, 3588
83. Wang, J.L. *et al.* (2018) Dissection of DNA double-strand-break repair using novel single-molecule forceps. *Nat. Struct. Mol. Biol.* 25, 482–487
84. De Bragança, S. *et al.* (2023) APLF and long non-coding RNA NIHCOLE promote stable DNA synapsis in non-homologous end joining. *Cell Rep.* 42, 111917
85. Graham, T.G.W. *et al.* (2016) Two-stage synapsis of DNA ends during non-homologous end joining. *Mol. Cell* 61, 850–858
86. Carney, S.M. *et al.* (2020) XLF acts as a flexible connector during non-homologous end joining. *eLife* 9, e61920
87. Chen, S. *et al.* (2021) Structural basis of long-range to short-range synaptic transition in NHEJ. *Nature* 593, 294–298
88. Chaplin, A.K. *et al.* (2021) Cryo-EM of NHEJ supercomplexes provides insights into DNA repair. *Mol. Cell* 81, 3400–3409
89. Chaplin, A.K. *et al.* (2021) Dimers of DNA-PK create a stage for DNA double-strand break repair. *Nat. Struct. Mol. Biol.* 28, 13–19
90. Buehl, C.J. *et al.* (2023) Two distinct long-range synaptic complexes promote different aspects of end processing prior to repair of DNA breaks by non-homologous end joining. *Mol. Cell* 83, 698–714
91. Stinson, B.M. *et al.* (2020) A mechanism to minimize errors during non-homologous end joining. *Mol. Cell* 77, 1080–1091
92. Brouwer, I. *et al.* (2016) Sliding sleeves of XRCC4–XLF bridge DNA and connect fragments of broken DNA. *Nature* 535, 566–569
93. Hammel, M. *et al.* (2011) XRCC4 protein interactions with XRCC4-like factor (XLF) create an extended grooved scaffold for DNA ligation and double strand break repair. *J. Biol. Chem.* 286, 32638–32650
94. Hammel, M. *et al.* (2010) XLF regulates filament architecture of the XRCC4·ligase IV complex. *Structure* 18, 1431–1442
95. Bergstrand, S. *et al.* (2022) Small Cajal body-associated RNA 2 (scaRNA2) regulates DNA repair pathway choice by inhibiting DNA-PK. *Nat. Commun.* 13, 1015
96. Thapar, R. *et al.* (2020) Mechanism of efficient double-strand break repair by a long non-coding RNA. *Nucleic Acids Res.* 48, 10953–10972
97. Unfried, J.P. *et al.* (2021) Long noncoding RNA NIHCOLE promotes ligation efficiency of DNA double-strand breaks in hepatocellular carcinoma. *Cancer Res.* 81, 4910–4925
98. Wang, D. *et al.* (2020) LRIK interacts with the Ku70–Ku80 heterodimer enhancing the efficiency of NHEJ repair. *Cell Death Differ.* 27, 3337–3353
99. Conlin, M.P. *et al.* (2017) DNA ligase IV guides end-processing choice during nonhomologous end joining. *Cell Rep.* 20, 2810–2819
100. Reid, D.A. *et al.* (2017) Bridging of double-stranded breaks by the nonhomologous end-joining ligation complex is modulated by DNA end chemistry. *Nucleic Acids Res.* 45, 1872–1878
101. Stinson, B.M. *et al.* (2022) Structural role for DNA Ligase IV in promoting the fidelity of non-homologous end joining. *BioRxiv* Published online October 26, 2022. https://doi.org/10.1101/2022.10.26.513880
102. Miller, H. *et al.* (2017) Single-molecule techniques in biophysics: a review of the progress in methods and applications. *Rep. Prog. Phys.* 81, 024601
103. De Vlaminck, I. and Dekker, C. (2012) Recent advances in magnetic tweezers. *Annu. Rev. Biophys.* 41, 453–472
104. Neuman, K.C. and Nagy, A. (2008) Single-molecule force spectroscopy: optical tweezers, magnetic tweezers and atomic force microscopy. *Nat. Methods* 5, 491–505
105. Baró, A.M., Reifenberger, R.G., eds (2012) *Atomic Force Microscopy in Liquid: Biological Applications*, Wiley
106. Strick, T.R. *et al.* (1996) The elasticity of a single supercoiled DNA molecule. *Science* 271, 1835–1837
107. Candelli, A. *et al.* (2011) Combining optical trapping, fluorescence microscopy and micro-fluidics for single molecule studies of DNA–protein interactions. *Phys. Chem. Chem. Phys.* 13, 7263–7272